MNRAS **000**, 1–21 (2015) Preprint 17 December 2015 Compiled using MNRAS LATEX style file v3.0

The circum-galactic medium of quasars: CIV absorption systems.

M. Landoni,[1⋆] R. Falomo,[2] A. Treves,[3] R. Scarpa,[4] E. P. Farina[5]
[1] *INAF - Osservatorio Astronomico di Brera, via E. Bianchi 46 Merate (LC)*
[2] *INAF - Osservatorio Astronomico di Padova, vicolo dell'Osservatorio 5 Padova (PD)*
[3] *Universita' degli Studi dell'Insubria, via Valleggio 11 Como (CO)*
[4] *Instituto de Astrofisica de Canarias - IAC*
[5] *Max–Planck–Institut für Astronomie — Königstuhl 17, D-69117 Heidelberg, Germany*

arXiv:1512.05115v1 [astro-ph.GA] 16 Dec 2015

17 December 2015

ABSTRACT

We investigate the properties of the circumgalactic gas in the halo of quasar host galaxies from CIV absorption line systems. Optical spectroscopy of closely aligned pairs of quasars (projected distance $\leq$ 200 kpc) obtained at the Gran Telescopio Canarias is used to investigate the distribution of the absorbing gas for a sample of 18 quasars at z $\sim$ 2. We found that the detected absorption systems of EW $\geq$ 0.3Å associated with the foreground QSO are revealed up to 200 kpc from the center of the host galaxy. The structure of the absorbing gas is rather patchy with a covering fraction of the gas that quickly decreases beyond 100 kpc. These results are in qualitative agreement with those found for the lower ionisation metal Mg II λ2800Å.

Key words: quasars - C IV absorptions systems - Intervening absorptions - QSO host galaxies

1 INTRODUCTION

Direct observation of low redshift galaxies ($z \leq 1$) demonstrated the presence of large and diffuse warm-to-hot gas halos up to $\sim$ 200 kpc commonly referred as circumgalactic-medium (CGM), see e.g. Lanzetta et al. (1995); Chen et al. (2001); Churchill et al. (2005). In the last decades, a number of papers exploited absorption lines imprinted in the spectra of background QSO to investigate the physical properties of the CGM (e.g. Bahcall & Spitzer 1969; Churchill et al. 2005; Nielsen et al. 2013a,b) finding significant correlation between the absorptions of the gas in CGM and the global properties of galaxies, such as luminosity (Chen & Tinker 2008), mass (Churchill et al. 2013) , color (Zibetti et al. 2007) and star formation rate (Prochter et al. 2006; Ménard et al. 2011; Nestor et al. 2011). Nevertheless, only a few studies have been focused on the properties of the gaseous halo of galaxies hosting a QSO in their centre (Hennawi et al. 2006; Hennawi & Prochaska 2007, and references therein).

The standard model for the origin of the extreme luminosity of quasars (QSO) considers that a supermassive black hole shines when intense mass inflow takes place, possibly as a consequence of tidal forces in dissipative events (Di Matteo et al. 2005). In this scenario, the CGM of QSO is expected to be populated by tidal debris, streams, and cool gas clouds, as commonly observed in interacting galaxies (see e.g. Sulentic et al. 2001; Cortese et al. 2006). Moreover the gas of the CGM belonging to the QSO host galaxy could be metal enriched by supernova-driven winds triggered by starbursts events associated to the mergers or by QSO-driven outflows of gas (e.g., Steidel et al. 2010; Shen & Ménard 2012). Although in the last few years a great effort allowed to detect emission lines that arise from the CGM (Hennawi & Prochaska 2013; Martin et al. 2014; Cantalupo et al. 2014; Hennawi et al. 2015), only the Lyman-α feature has been observed so far. For these reasons, the most efficient way to study the CGMs is to investigate the absorption features that it imprints in the spectra of background QSOs (e.g., Adelberger et al. 2005; Hennawi et al. 2006).

In this context projected QSO pairs are ideal observational tools for this purpose, since the light of the very bright source in the background ($z = z_B$), goes through the extended halo of the foreground ($z_F < z_B$) object (e.g., Hennawi et al. 2006; Farina et al. 2013). The absorption features in the gaseous halos belonging to the foreground QSO can be therefore exploited to understand the processes of enrichment of material far from the host galaxy. In this paper we aim to characterise the properties of intervening C IV absorbers in the circumgalactic medium of quasars host galaxies up to a projected distance (PD) of 200 kpc. We

⋆ E-mail: marco.landoni@brera.inaf.it

© 2015 The Authors

adopt the following cosmological parameters $H_0 = 70$ km s^{-1} Mpc^{-1}, $\Omega_m = 0.27$, $\Omega_\Lambda = 0.73$.

2 SAMPLE SELECTION

In order to investigate the properties and abundances of C IV in the CGM of quasars, we selected QSO projected pairs by searching in Sloan Digital Sky Survey DR10 of spectroscopic quasars (Paris et. al. 2012). We assume as good candidates pairs with PD (comoving transverse distance) smaller than 200 kpc in order to characterise the innermost region of the CGM. Further, we constrain the line-of-sight (LOS) velocity difference, based on the published redshift, $\Delta V \geq 5000$ km s^{-1} to ensure that pairs are not gravitationally bound. We also put a threshold on the magnitude of the background QSO ($m_r \leq 20$) to secure spectra with adequate signal to noise ratio (≥ 15) and on declination to ensure good visibility from Roque de los Muchachos observatory. Finally, we selected pairs in which the redshifts of the foreground and background QSOs combine, so that the CIV absorption lines at the redshift of the foreground (z_F) fall within the wavelength range 4500-6000Å. This procedures yielded 34 candidate pairs. We selected 25 objects for observation, according to the visibility of the considered period. However, only 18 targets were obtained due to partially bad weather conditions. Details on the observed objects are reported in Table 1.

3 OBSERVATIONS, DATA REDUCTION AND DATA ANALYSIS

We observed our QSO pairs with the 10.4m Gran Telescopio Canarias (GTC) equipped with the Optical System for Imaging and Low Resolution Integrated Spectroscopy (OSIRIS, Cepa et al. (2003)) from September 2013 to August 2014. Observations were gathered with GTC-OSIRIS adopting the grism R2500V with a slit of 1.00″ yielding a resolution $\frac{\lambda}{\Delta\lambda} \sim 2500$ (1 px = 0.80 Å, corresponding to 45 km s^{-1} at center wavelength). In this case the resolution corresponds to a FWHM of about 2 Å allowing to fully resolve the components of the C IV doublets ($\lambda\lambda$1548-1551Å). The resolution element, which corresponds to a FWHM of 120 km s^{-1}, is not sufficient to kinematically resolve the internal dynamics of the absorbing gas which is beyond the aim of our investigation. For each pair we oriented the slit in order to acquire simultaneously the spectra of the two objects and we secured three different exposures, applying a small shift of 5″ along the slit to better reject cosmic rays and for accounting for CCD defects.

We reduced our data by the adoption of standard `IRAF`[1] procedures. Briefly, for each frame, we performed bias subtraction and flat field correction using the `ccdred` package. Wavelength calibration has been assessed through the observation of arc lamps (Xe+Ne+HgAr) and the residuals on the calibration are around 0.04Å. We flux calibrated the spectra exploiting standard stars observed during the same nights of the targets. We corrected for systematics, slit losses and variation of the sky conditions through aperture photometry of the field, in r'-band, acquired shortly before the observation. We report an example of spectra of a pair in Figure 1 and we give the full figure set in the electronic edition of this Journal. The Galactic reddening was taken into account considering the estimates from Schlegel et al. (1998) assuming $R_V = 3.1$ (Cardelli et al. 1989). In the spectra of the QSO presented in Figure 1, in addition to the typical broad emission lines of C IV and C III], we note that several absorptions lines due to intervening matter (e.g. Mg II at $z = 0.869$) are present. The C IV absorption system ascribed to the halo of the foreground QSO is also detected in some cases in the spectrum of the background one.

We performed the search of the C IV ($\lambda\lambda$1548 − 1550) absorption doublet in the spectrum of the background QSO for each pair in an interval of wavelengths corresponding to 4000 km s^{-1} centered at the expected position of C IV lines at the redshift of the foreground quasar. In the case of detection we fit the components by the adoption of two gaussian profiles, as illustrated in the boxes of Figure 2. Furthermore, in order to proper characterise the quality of the data, on each window we measured the minimum detectable Equivalent Width (EW_{min}) by following procedure described in Sbarufatti et al. (2006). Briefly, we evaluated the EW on bins of the size of the resolution element in various regions of the spectrum excluding telluric structures. We assume as EW_{min} the 2-σ deviation from the mean of the average of the distribution of the EWs obtained in each bin. Finally, concerning the LOS velocities of the detected C IV absorptions, we considered that the systems is associated to the foreground object only if $|\Delta V| \leq 500 - 600$ km s^{-1} rest frame. Results of our procedures are reported in Table 2.

4 RESULTS AND DISCUSSION

In 6 out of 18 pairs we detected C IV absorption system associated to the foreground QSO halo (see Table 2 and Figure 2). In one case (QQ09) we have a suggestion of a double C IV systems probably associated to two or more moving clouds belonging to the foreground QSO halos. In this case we deblended the features by fitting the four components adopting gaussian profiles (see box 4 of Figure 2). We also note that in QQ10 a C IV absorptions is detected at $\lambda \sim 4800$Å in the spectrum of background quasars, but we do not include it in our statistic since the velocity difference is slightly beyond our threshold. The EW of the detected associated C IV absorption systems together with the upper limits are shown in Figure 3 as a function of the projected separation from the foreground QSO. In spite of the relatively small statistics, considering both the detections and the upper limits, there is an indication that the absorbing systems decrease in intensity as a function of the distance from the center of the (foreground) quasars and that the absorbing gas becomes more patchy. We performed a Cox Proportional Hazard test including the uppers limits (Isobe et al. 1986) and found that the two quantities (PD and EW) are anti-correlated with a probability of $\sim 93\%$. This behaviour is qualitatively very similar (see Figure 3) to that of Mg II λ2800Å intervening systems (Farina et al. 2013, 2014) although the average red-

[1] IRAF is distributed by the National Optical Astronomy Observatories, which are operated by the Association of Universities for Research in Astronomy, Inc., under cooperative agreement with the National Science Foundation.

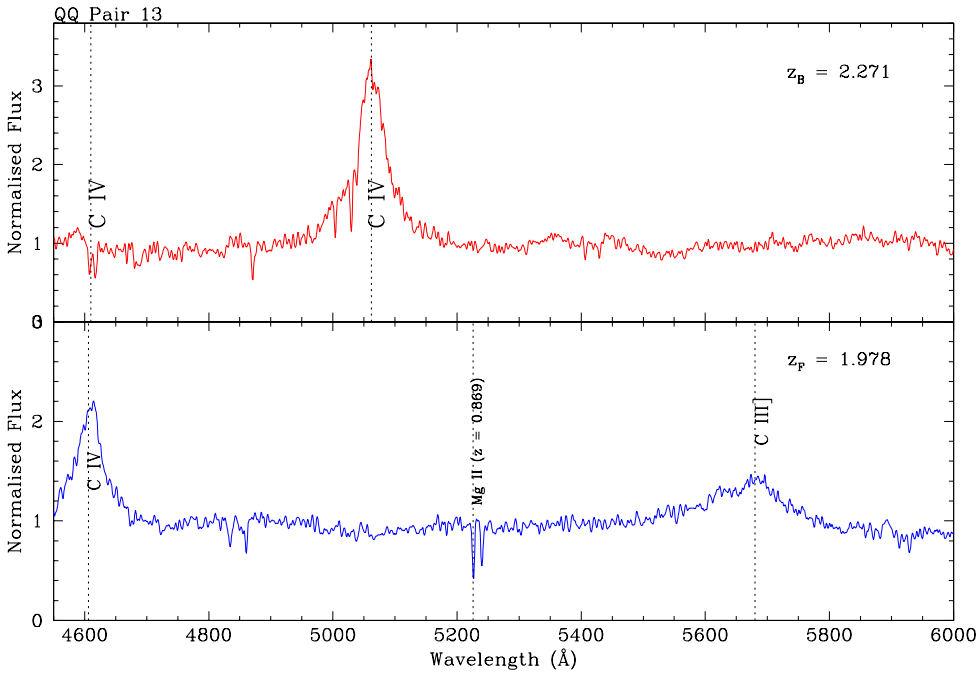

Figure 1. Normalised spectra of the pair QQ 13. Solid blue line is the spectrum of the foreground QSO while red solid line is used for the background one. The most prominent quasar emission lines are also marked. In the spectrum of the foreground we also detect an intervening Mg II absorption system at $z = 0.869$. The whole figure set is available in Electronic Version in the online edition of this Journal.

Table 1. Properties of the observed pairs. Pair identification (ID), position of the foreground target (RA,DEC), foreground redshift (z_F), background redshift (z_B), V apparent magnitudes of foreground and background QSO (V_F, V_B), Projected distance in kpc (PD), Signal to noise ratios (per pixel) of foreground and background object (SN_F, SN_B).

ID	RA_F	DEC_F	z_F	z_B	V_F	V_B	PD	SN_F	SN_B
QQ01	08:45:13.57	+39:10:25.65	2.040	2.210	19.8	19.5	180	15	15
QQ02	09:17:06.47	+00:56:35.10	2.140	2.472	20.4	20.2	200	10	10
QQ03	10:13:01.20	+40:23:03.52	2.185	2.504	18.4	19.2	192	35	20
QQ04	12:06:51.22	+02:04:21.90	2.443	2.522	20.5	19.0	110	15	20
QQ05	13:58:06.09	+61:18:26.70	2.015	2.167	20.5	20.2	190	10	15
QQ06	14:30:33.61	-01:34:45.69	2.273	2.350	19.5	19.5	55	10	10
QQ07	09:13:23.31	+04:02:35.15	2.040	2.375	19.1	19.5	92	15	15
QQ08	09:16:11.20	-01:19:41.50	2.753	2.917	20.7	20.8	87	15	10
QQ09	10:09:35.86	+47:49:34.61	2.292	2.590	20.7	19.7	93	5	15
QQ10	11:34:26.18	+00:38:54.86	2.209	2.365	20.4	19.6	90	15	20
QQ11	00:42:52.23	+01:11:55.62	2.027	2.084	18.7	18.9	70	30	30
QQ12	03:44:11.98	+00:09:27.88	2.125	2.240	21.4	19.4	184	10	25
QQ13	12:14:31.06	+32:23:28.24	1.978	2.271	19.5	20.0	202	10	10
QQ14	08:45:33.63	+25:15:51.64	2.110	2.292	19.0	20.3	186	15	5
QQ15	12:19:30.15	+15:10:28.44	1.943	2.313	19.2	19.7	110	35	25
QQ16	12:21:49.62	+37:00:13.82	2.119	2.322	20.4	20.7	97	10	10
QQ17	14:59:06.93	+12:34:49.54	2.109	2.500	18.6	20.6	42	50	20
QQ18	15:53:19.30	+31:52:40.39	2.817	3.194	22.3	20.0	200	15	25

shift of the objects is somewhat different ($< z >= 1.2$ for Mg II compared with $< z >= 2.1$ for C IV).

In order to quantify the patchy structure of the absorbing gaseous halos, we investigate the covering fraction of (f_c) of C IV in function of PD. We choose a threshold equivalent width $EW_{th} = 0.30$Å, which allows one to consider spectra with $EW_{min} \leq 0.25$Å except for one case (QQ14), and two bins of [0-100] kpc and [100-200] kpc. We define for each bin the f_c as the ratio between detected systems over the total number of pairs in the bin. Since the analysis of the covering fraction is sensitive to binning effect and depends on the adopted EW_{th}, we combine our results adopting the same EW_{th} for consistency with those recently drawn in the sample of Prochaska et al. (2014) yielding 7 extra sources. We find that the covering fraction for C IV is f_c ($\geq$0.30) $= 0.63^{+0.10}_{-0.12}$ for the bin [0-100] kpc while for the case of [100-200] kpc is f_c ($\geq$ 0.30Å) $= 0.25^{+0.10}_{-0.08}$ (see Figure 4).

Table 2. Measurement of the C IV absorption in the background QSO of each pair. Identification label (ID), CIV 1548-1551λ observed wavelength and equivalent widths (rest), Doublet Ratio (DR), Velocity difference between the absorption redshift and the foreground QSO redshift. ΔV (km s^{-1}), Equivalent width minimum detectable on the spectrum (Å).

ID	$\lambda_{\rm abs}$(1548) [Å]	W (1548) [Å]	$\lambda_{\rm abs}$(1551) [Å]	W (1551) [Å]	DR	ΔV [km s^{-1}]	EW$_{min}$ [Å]
QQ01B	-	-	-	-	-	-	0.13
QQ02B	-	-	-	-	-	-	0.12
QQ03B	-	-	-	-	-	-	0.10
QQ04B	5324	0.70 ± 0.20	5334	0.30 ± 0.10	2.30	-300	0.15
QQ05B	-	-	-	-	-	-	0.20
QQ06B	5075	1.30 ± 0.40	5084	0.60 ± 0.20	2.17	500	0.15
QQ07B	-	-	-	-	-	-	0.20
QQ08B	5805	0.50 ± 0.20	5817	0.30 ± 0.10	1.67	-500	0.25
QQ09B	5114	0.60 ± 0.20	5124	0.30 ± 0.10	2.00	600	0.18
QQ10B	-	-	-	-	-	-	0.20
QQ11B	-	-	-	-	-	-	0.16
QQ12B	-	-	-	-	-	-	0.10
QQ13B	4607	0.50 ± 0.20	4616	0.40 ± 0.15	1.25	-400	0.23
QQ14B	-	-	-	-	-	-	0.40
QQ15B	-	-	-	-	-	-	0.20
QQ16B	-	-	-	-	-	-	0.20
QQ17B	4824	0.50 ±0.10	4834	0.30 ± 0.05	1.67	600	0.20
QQ18B	-	-	-	-	-	-	0.18

Horizontal bars are the bin width while vertical bars are the 1-σ uncertainties in the f_c calculated upon the binomial statistics (68% Wilson score). We note that the f_c of C IV decreases of about a factor of two between the first bin (0-100 kpc) and the second one (100-200 kpc). It is of interest to compare these results with those derived from the covering fraction of the Mg II. We computed, assuming the same bins and EW$_{th}$, the f_c for the Mg II by adopting data presented in Farina et al. (2013, 2014) for 26 pairs. We found that f_c (≥ 0.30) $= 0.86^{+0.10}_{-0.09}$ for the bin [0-100] kpc and f_c (≥ 0.30Å) $= 0.45^{+0.13}_{-0.10}$ for [100-200] kpc (see Figure 4).

Both for Mg II and CIV species, the covering fraction of the absorbing material is halved from the region (< 100 kpc) close to the center of the host galaxy to the immediate outer region (100-200 kpc). There is a suggestion that the covering fraction of CIV absorbers is systematically smaller than that of MgII. This behaviour could be related due to different ionisation energies of the two species and/or due to chemical abundances. We note that, although the statistics is small, our finding is also consistent with results based on C II and C IV for a sample of 60 quasar pairs (Prochaska et al. 2014).

ACKNOWLEDGEMENTS

EPF acknowledges funding through the ERC grant 'Cosmic Dawn'.

REFERENCES

Adelberger, K. L., Shapley, A. E., Steidel, C. C., et al. 2005, ApJ, 629, 636
Bahcall, J. N., & Spitzer, L., Jr. 1969, ApJ, 156, L63
Cantalupo, S., Arrigoni-Battaia, F., Prochaska, J. X., Hennawi, J. F., & Madau, P. 2014, Nature,506, 63
Cardelli, J. A., Clayton, G. C., & Mathis, J. S. 1989, ApJ, 345, 245
Cepa, J., Aguiar-Gonzalez, M., Bland-Hawthorn, J., et al. 2003, Proc. SPIE, 4841, 1739
Chen, H.-W., Lanzetta, K. M., Webb, J. K., & Barcons, X. 2001, ApJ, 559, 654
Chen, H.-W., & Tinker, J. L. 2008, ApJ, 687, 745
Churchill, C., Steidel, C., & Kacprzak, G. 2005, Extra-Planar Gas, 331, 387
Churchill, C. W., Nielsen, N. M., Kacprzak, G. G., & Trujillo-Gomez, S. 2013, ApJ, 763, L42
Cortese, L., Gavazzi, G., Boselli, A., et al. 2006, A&A, 453, 847
Di Matteo, T., Springel, V., & Hernquist, L. 2005, Nature, 433, 604
Farina, E. P., Falomo, R., Decarli, R., Treves, A., & Kotilainen, J. K. 2013, MNRAS, 429, 1267
Farina, E. P., Falomo, R., Scarpa, R., et al. 2014, MNRAS, 441, 886
Hennawi, J. F., Prochaska, J. X., Burles, S., et al. 2006, ApJ, 651, 61
Hennawi, J. F., & Prochaska, J. X. 2007, ApJ, 655, 735
Hennawi, J. F., & Prochaska, J. X. 2013, ApJ, 766, 58
Hennawi, J. F., Prochaska, J. X., Cantalupo, S., & Arrigoni-Battaia, F. 2015, Science, 348, 779
Isobe, T., Feigelson, E. D., & Nelson, P. I. 1986, ApJ, 306, 490
Lanzetta, K. M., Bowen, D. V., Tytler, D., & Webb, J. K. 1995, ApJ, 442, 538
Martin, D. C., Chang, D., Matuszewski, M., et al. 2014, ApJ, 786, 106
Ménard, B., Wild, V., Nestor, D., et al. 2011, MNRAS, 417, 801
Nestor, D. B., Johnson, B. D., Wild, V., et al. 2011, MNRAS, 412, 1559
Nielsen, N.M., Churchill, C. W., Kacprzak, G. G., & Murphy, M. T. 2013, ApJ, 776, 114
Nielsen, N. M., Churchill, C. W., & Kacprzak, G. G. 2013, ApJ, 776, 115
Paris, I., Petitjean, P., Aubourg, É., et al. 2012, A&A, 548, A66
Prochaska, J. X., Lau, M. W., & Hennawi, J. F. 2014, ApJ, 796, 140
Prochter, G. E., Prochaska, J. X., & Burles, S. M. 2006, ApJ,

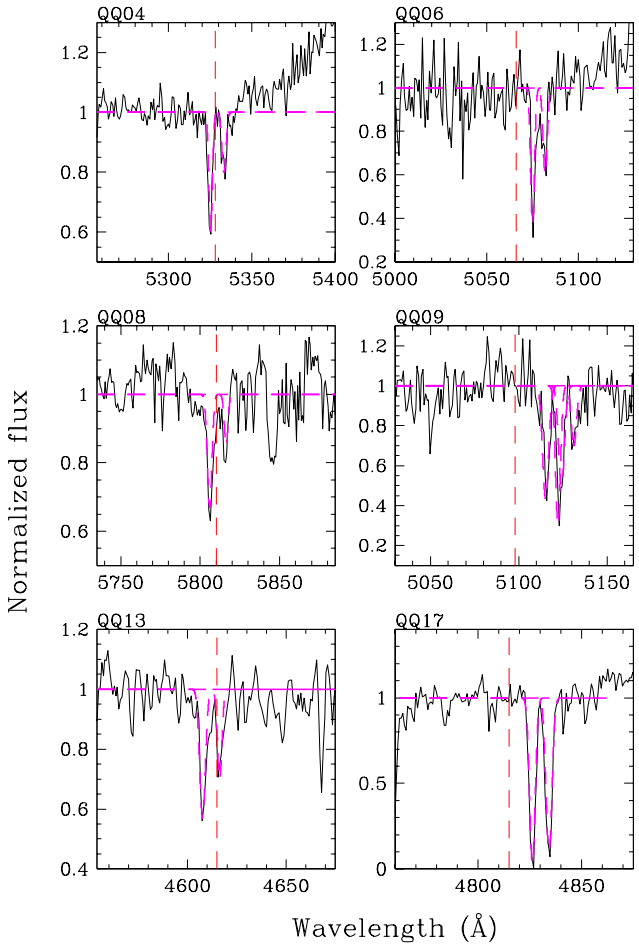

Figure 2. Normalized spectra of background quasars showing the intervening absorption feature identified as C IV 1548Å and C IV 1550Å that are close in velocity and projected distance form the foreground quasar (see text). The vertical dashed red line indicate the position of CIV 1548 emission line in the spectrum of the foreground QSO.

639, 766
Sbarufatti, B., Treves, A., Falomo, R., et al. 2006, AJ, 132, 1
Schlegel, D. J., Finkbeiner, D. P., & Davis, M. 1998, ApJ, 500, 525
Steidel, C. C., Erb, D. K., Shapley, A. E., et al. 2010, ApJ, 717, 289
Shen, Y., & Ménard, B. 2012, ApJ, 748, 131
Sulentic, J. W., Rosado, M., Dultzin-Hacyan, D., et al. 2001, AJ, 122, 2993
Zibetti, S., Ménard, B., Nestor, D. B., et al. 2007, ApJ, 658, 161

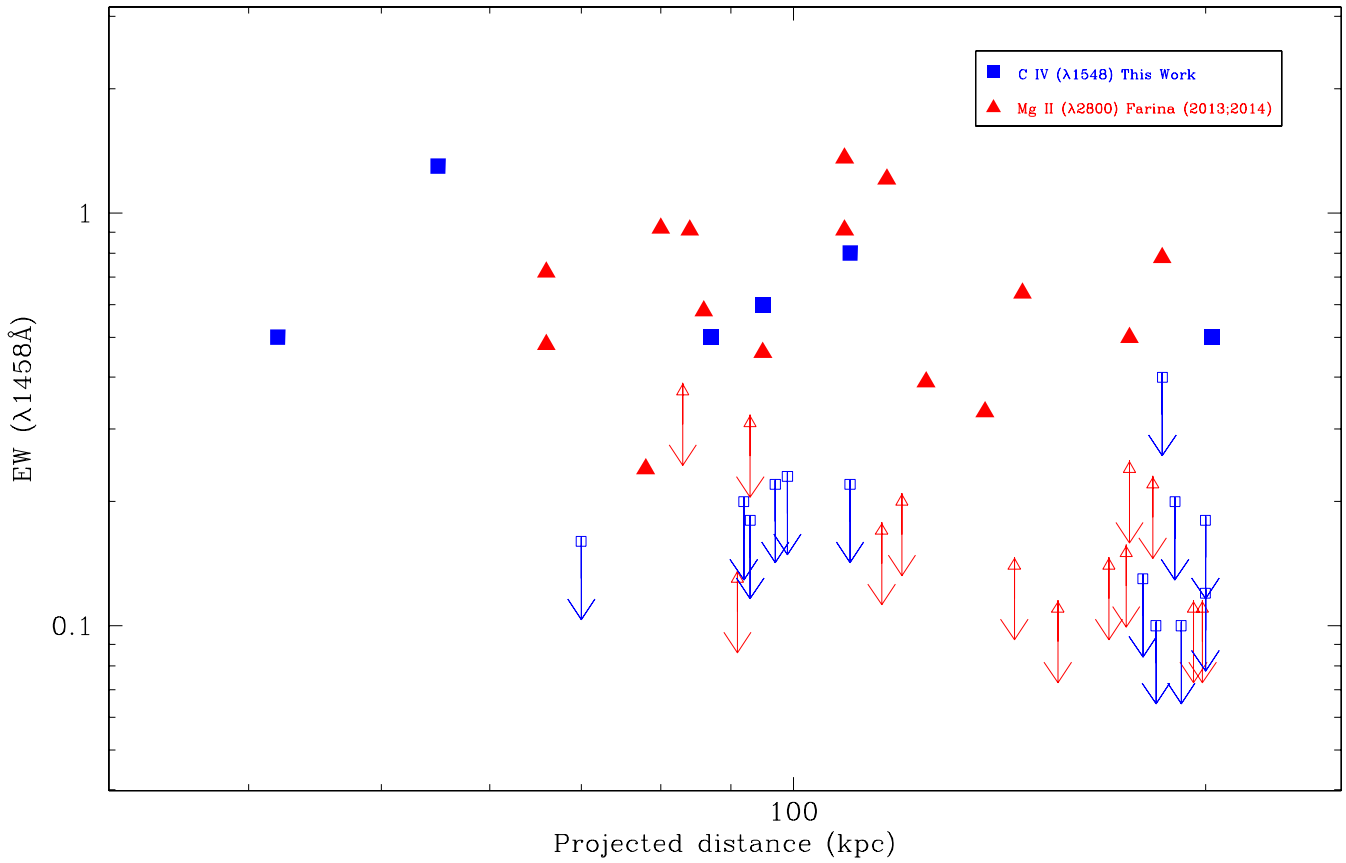

Figure 3. Equivalent width of C IV (filled blue squares) intervening absorption lines as a function of the projected distance from the quasar (including the upper limit of QQ10 from Farina et al 2013) . Upper limits are indicated by open squares with arrows (see text). Similar data for Mg II 2800 absorption systems (filled red triangles) and their relative upper limits (open triangles with arrows) (Farina et al. 2013, 2014).

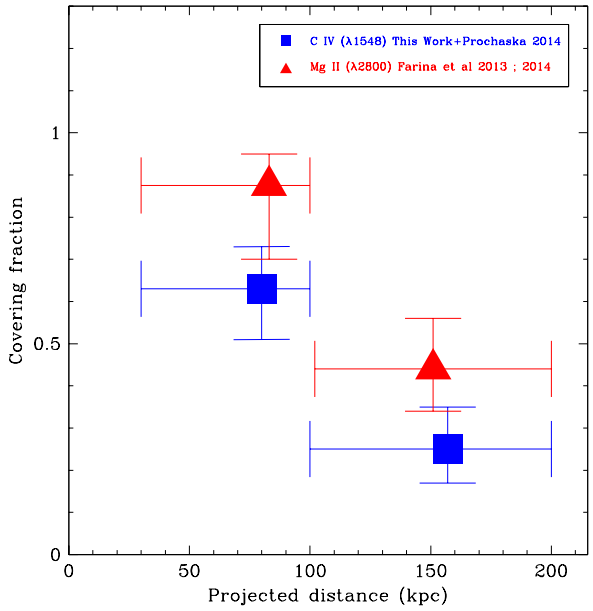

Figure 4. The covering fraction of C IV in QSO host galaxies (filled blue squares) derived from the combined sample (this work plus the dataset by (Prochaska et al. 2014), see text). For comparison we report the covering fraction of Mg II derived from the dataset considered in (Farina et al. 2013, 2014) (see text). Vertical error bar are 1-σ confidence level at 68% Wilson score for a binomial distribution.

QSO PAIRS SPECTRA FOR THE REFEREE DOCUMENTATION

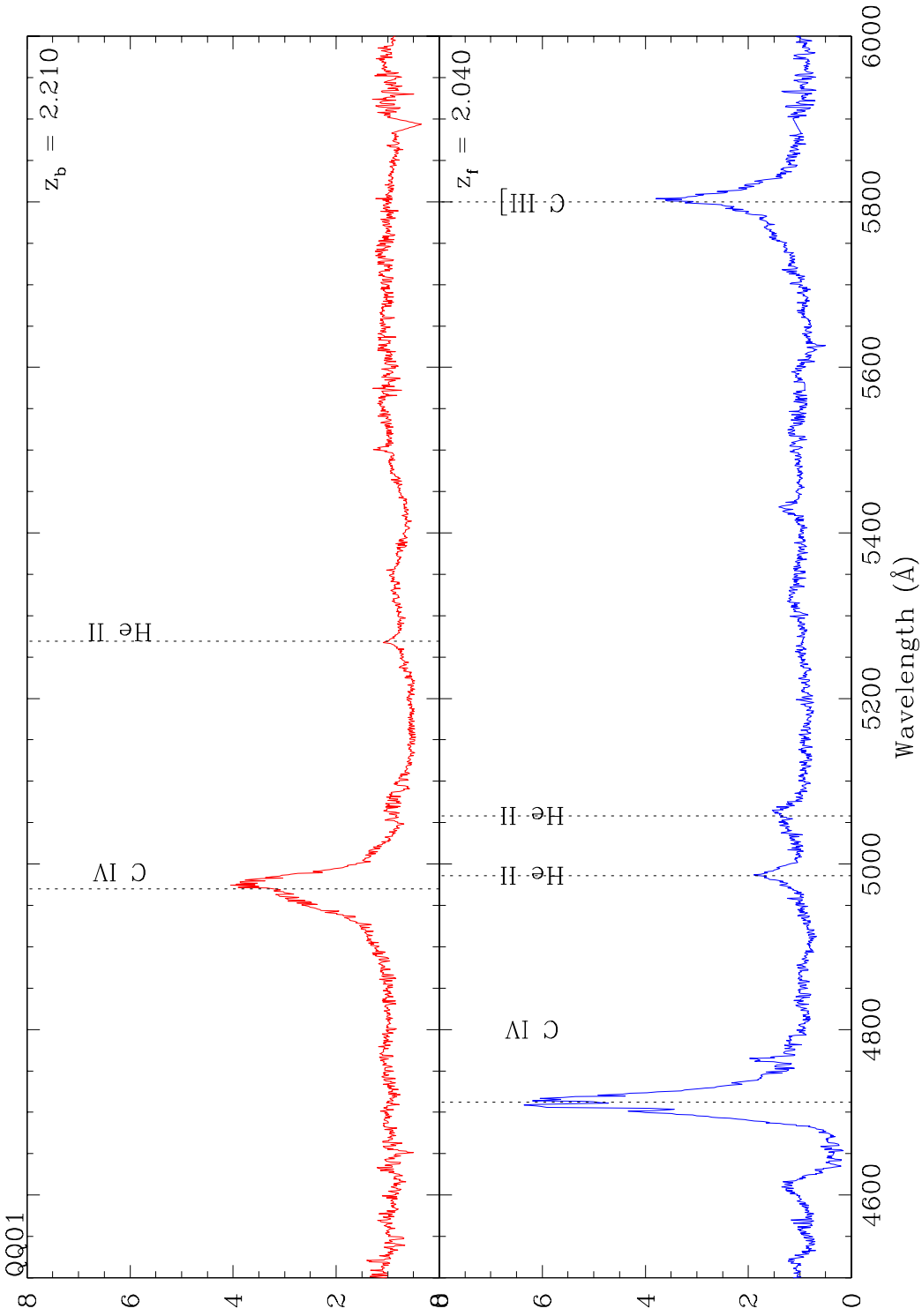

Figure 5. Spectra of pair QQ01.

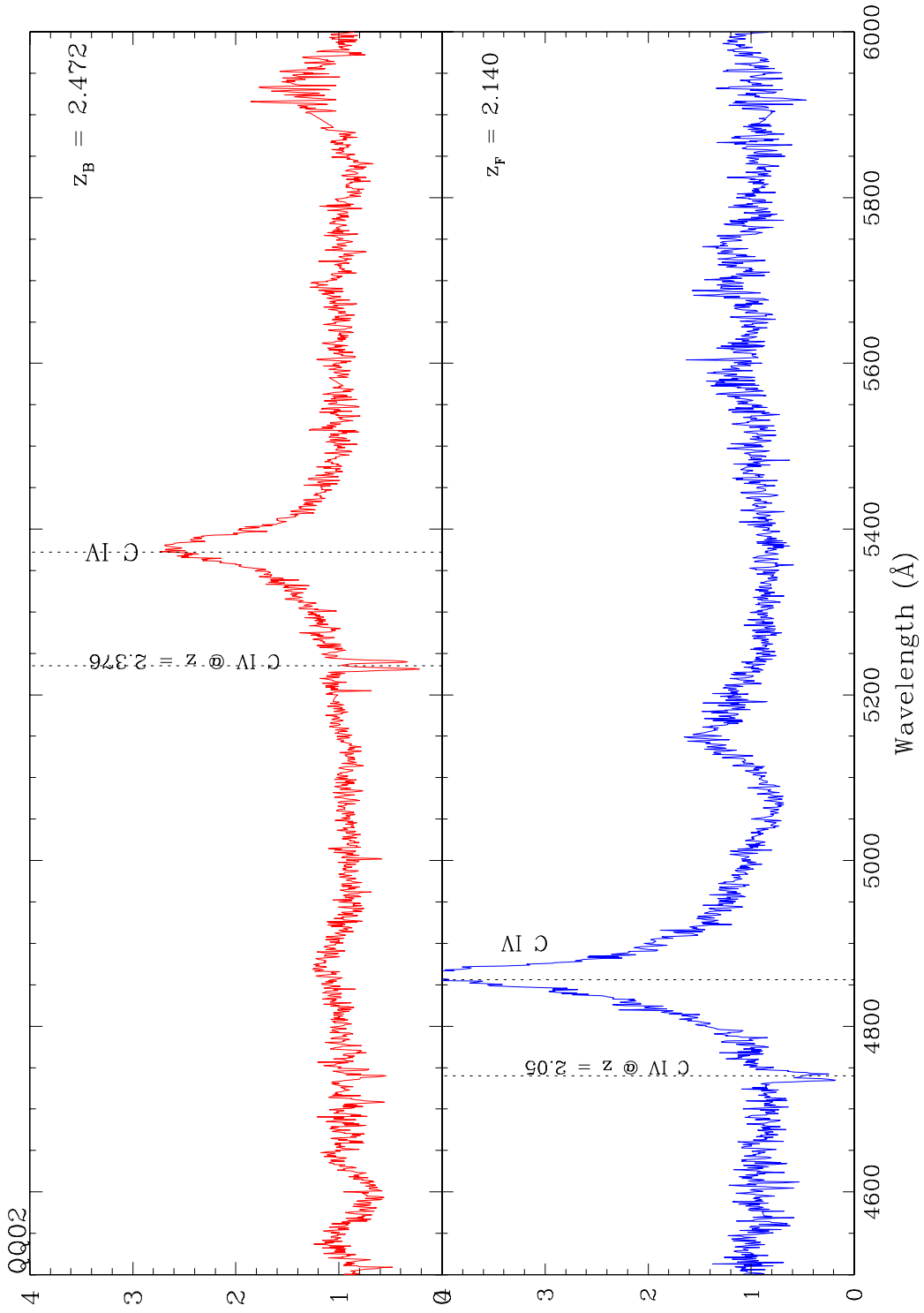

Figure 6. Spectra of pair QQ02.

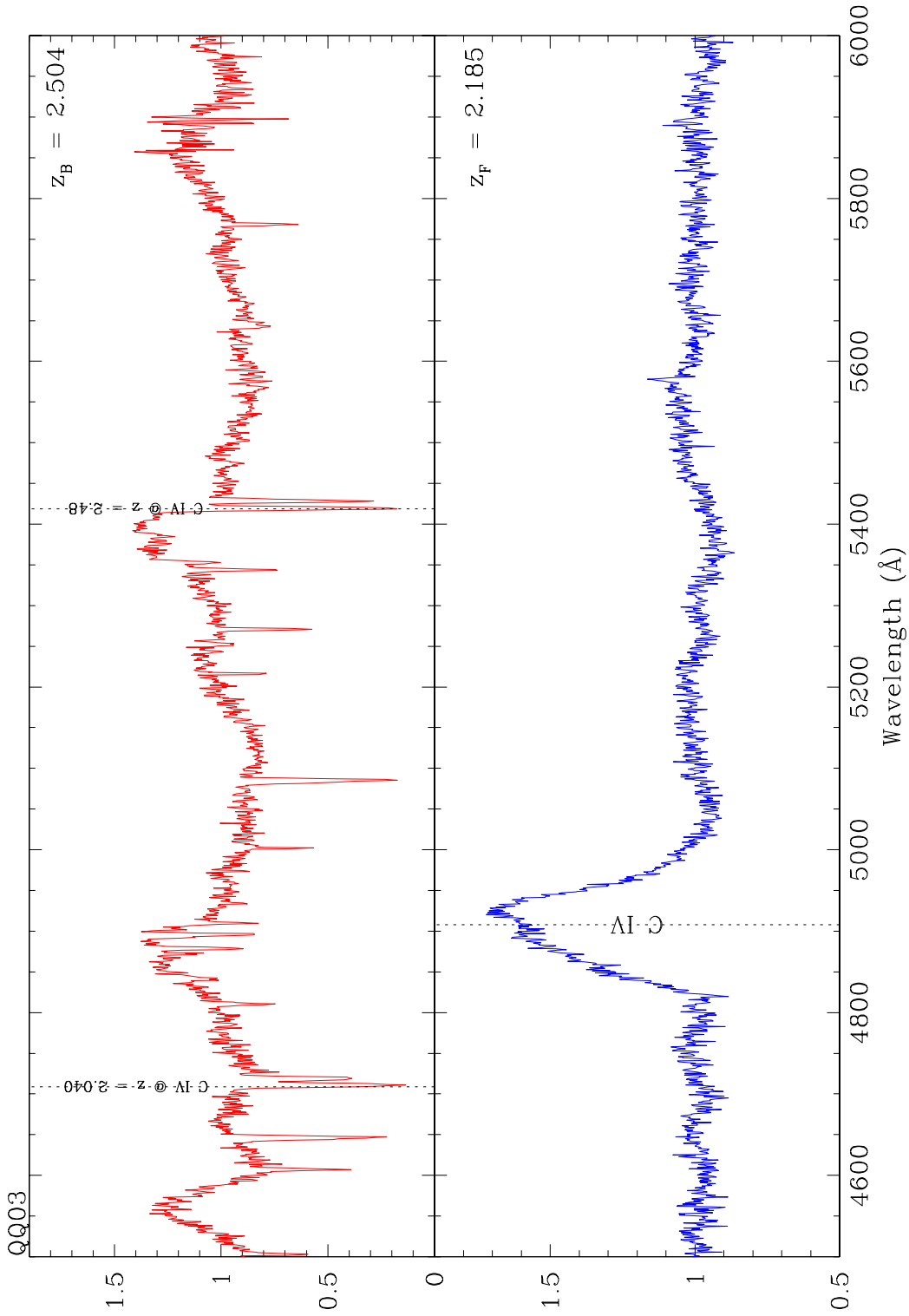

Figure 7. Spectra of pair QQ03.

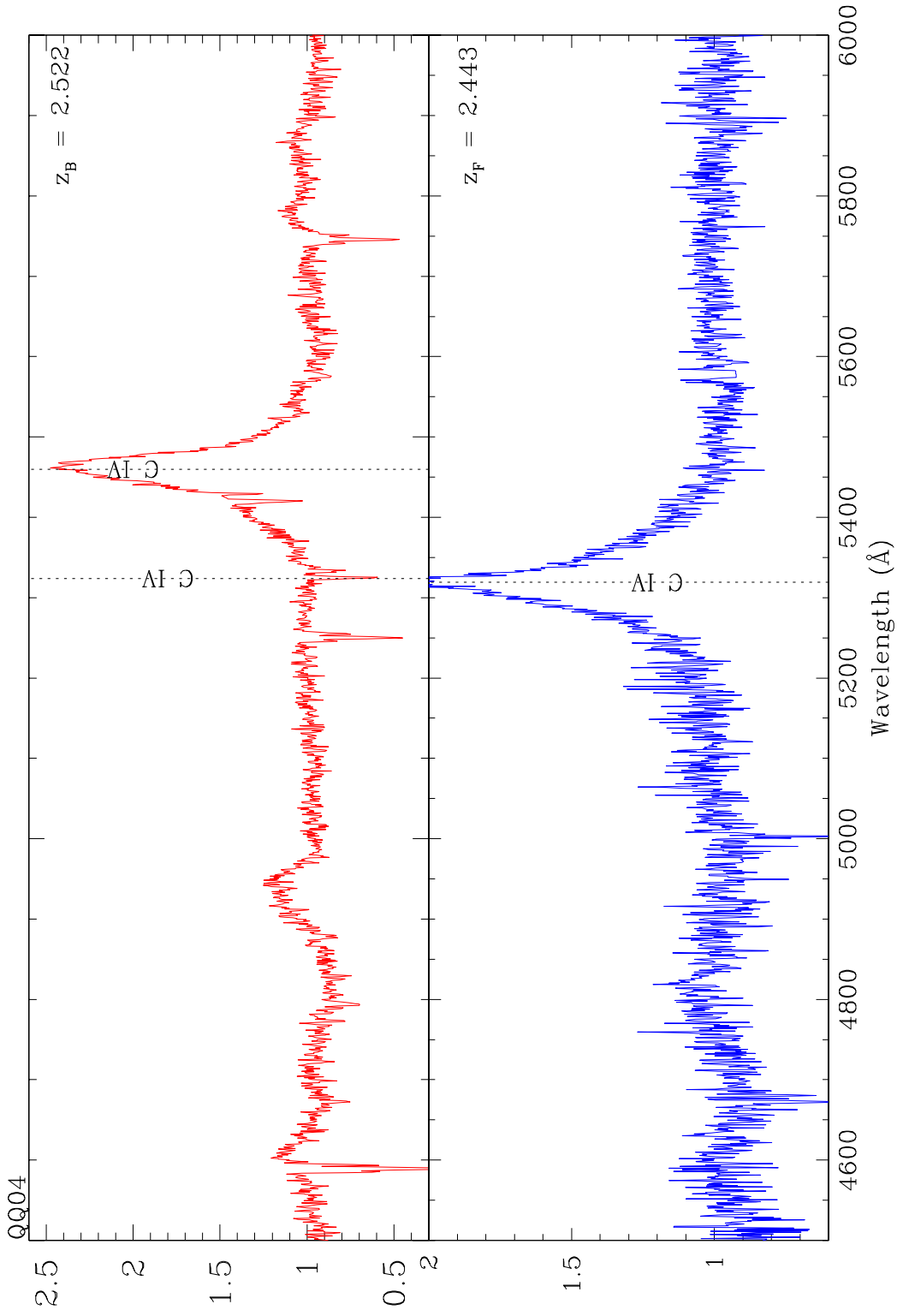

Figure 8. Spectra of pair QQ04.

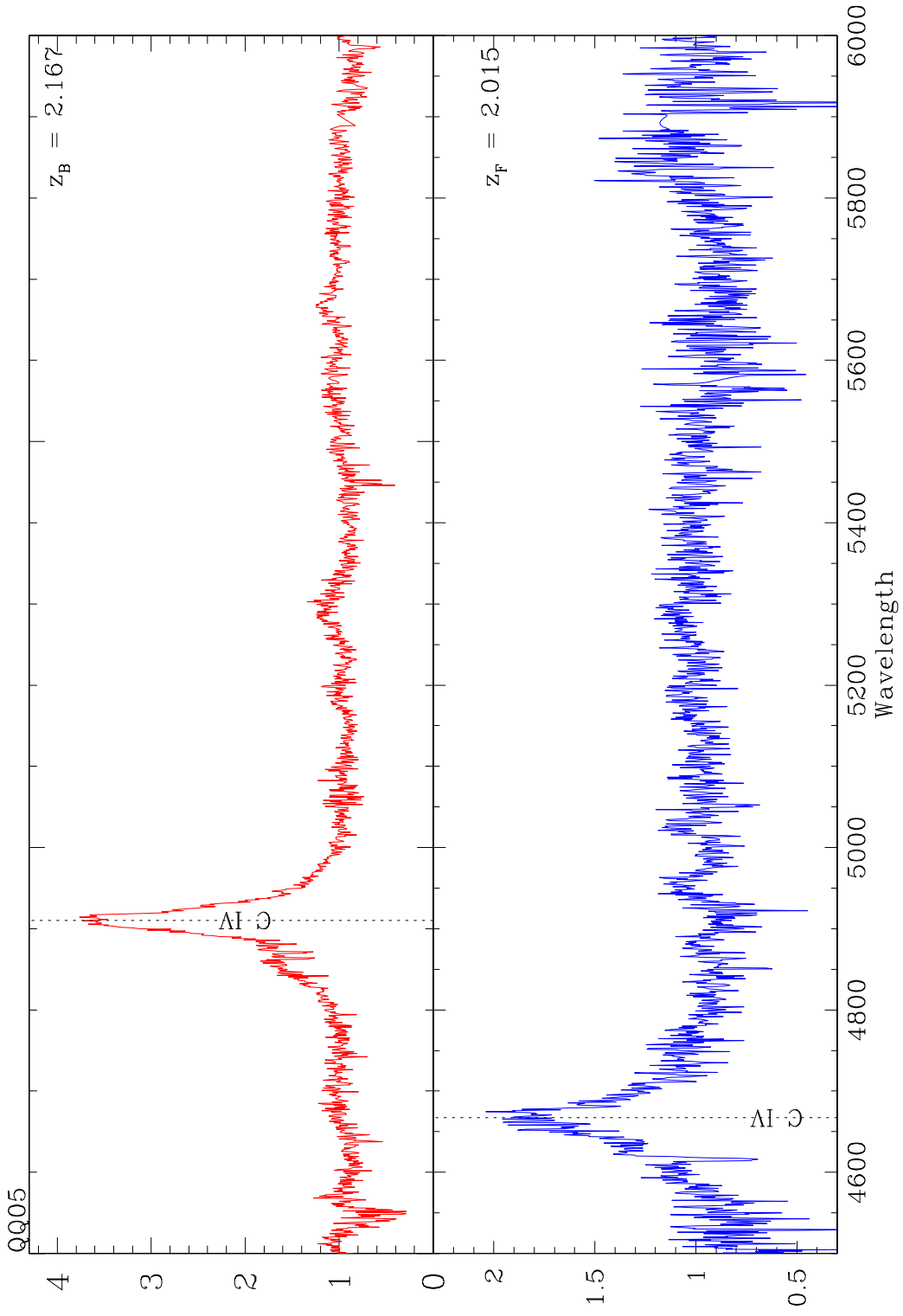

Figure 9. Spectra of pair QQ05.

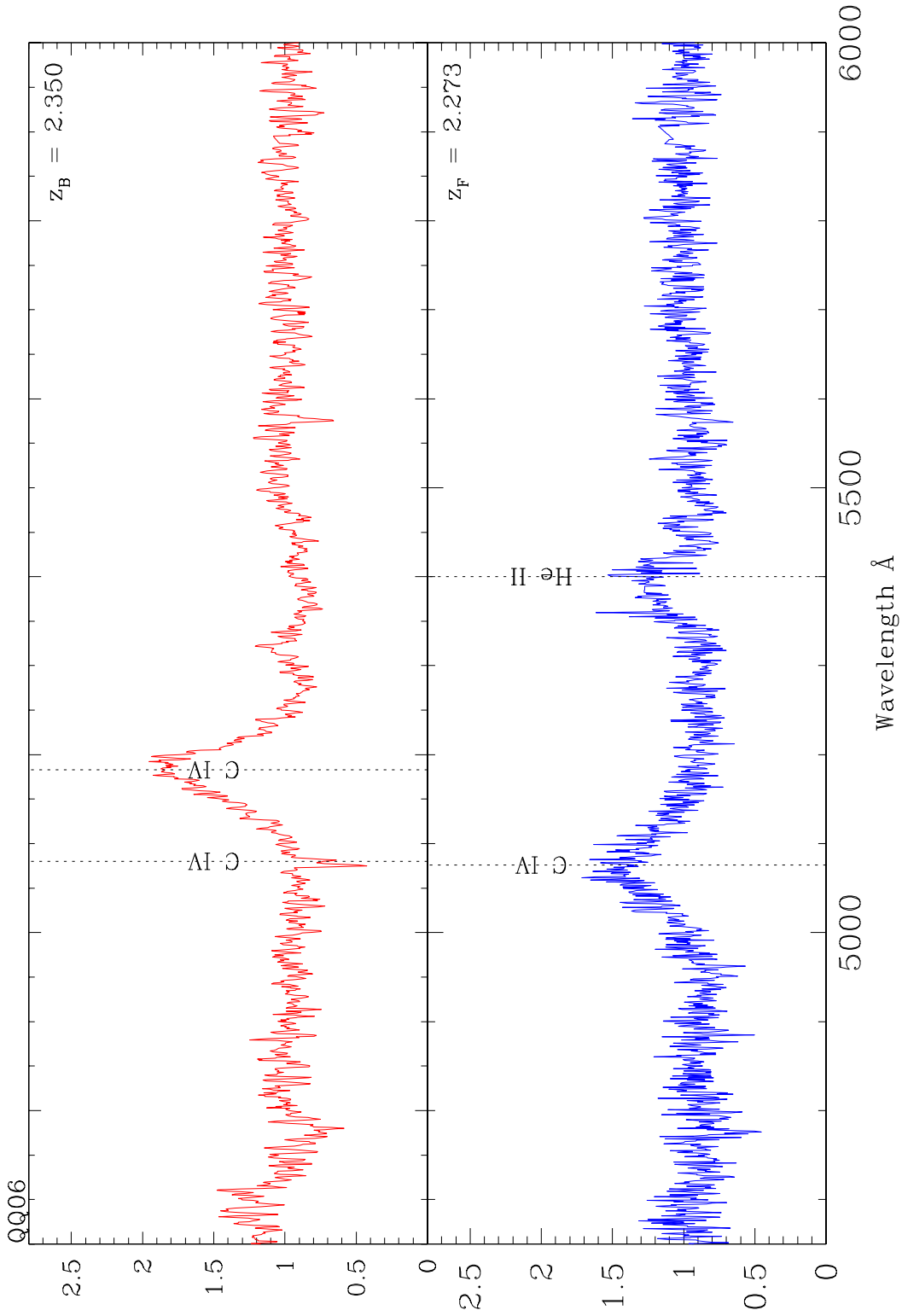

Figure 10. Spectra of pair QQ06.

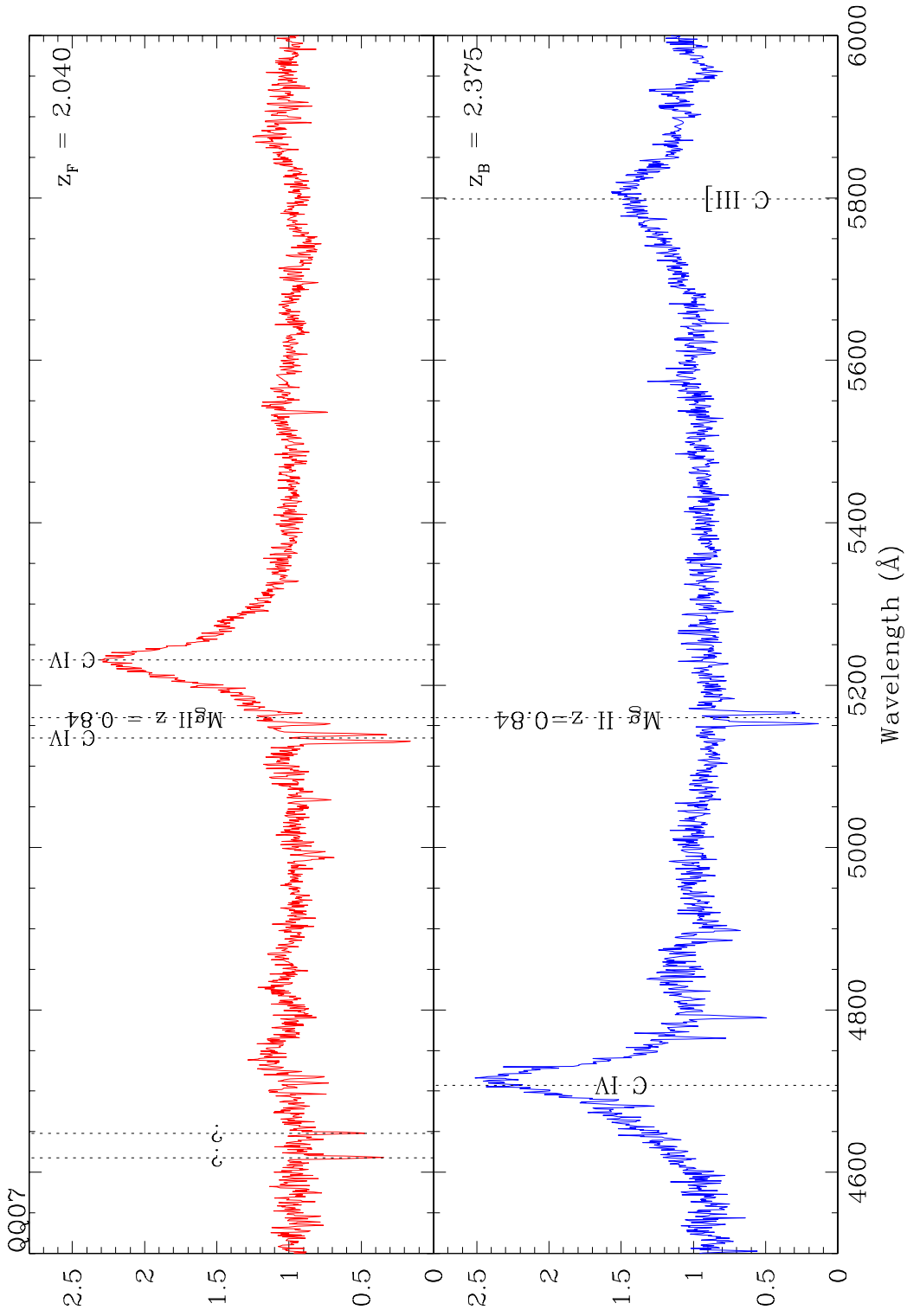

Figure 11. Spectra of pair QQ07.

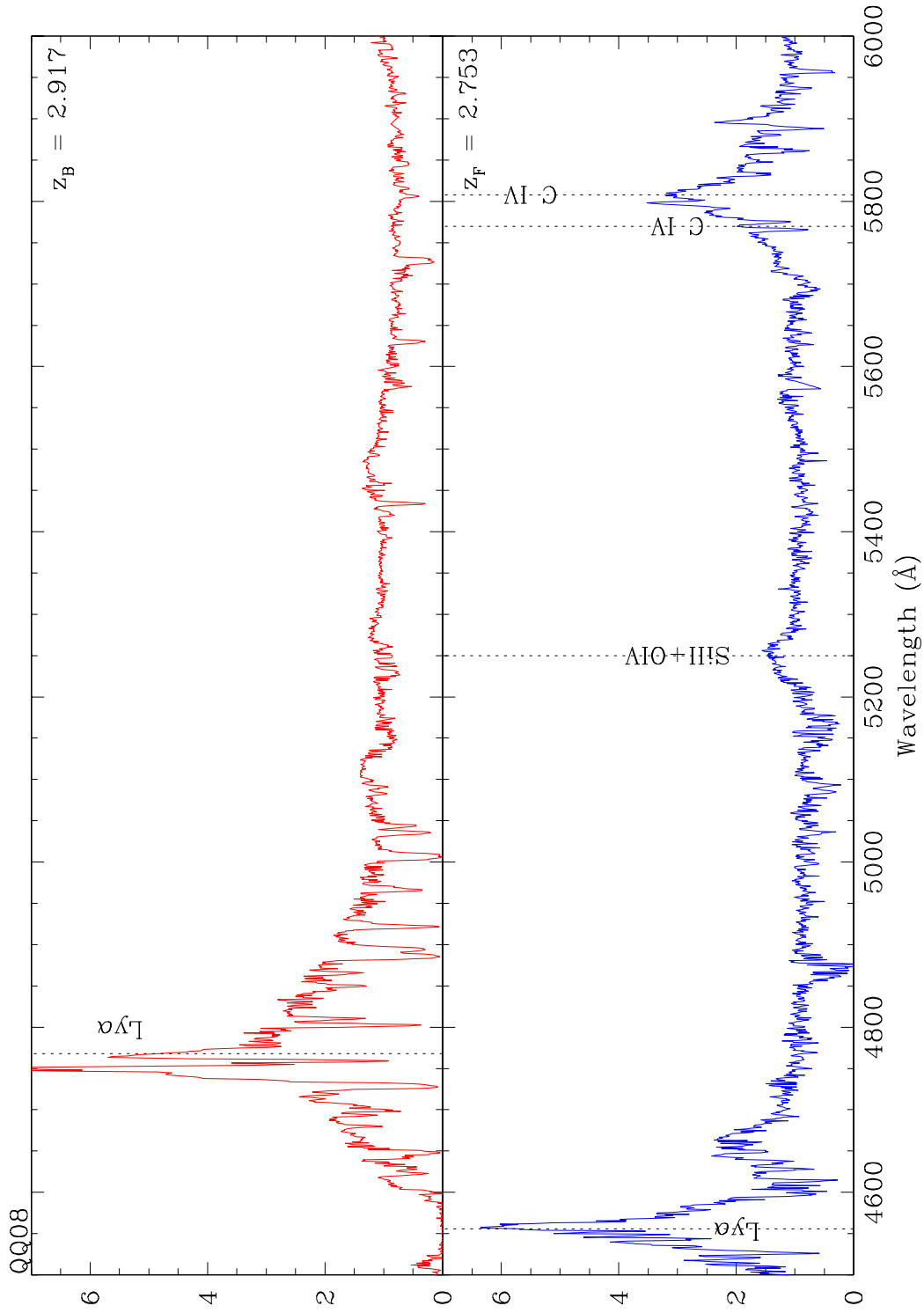

Figure 12. Spectra of pair QQ08.

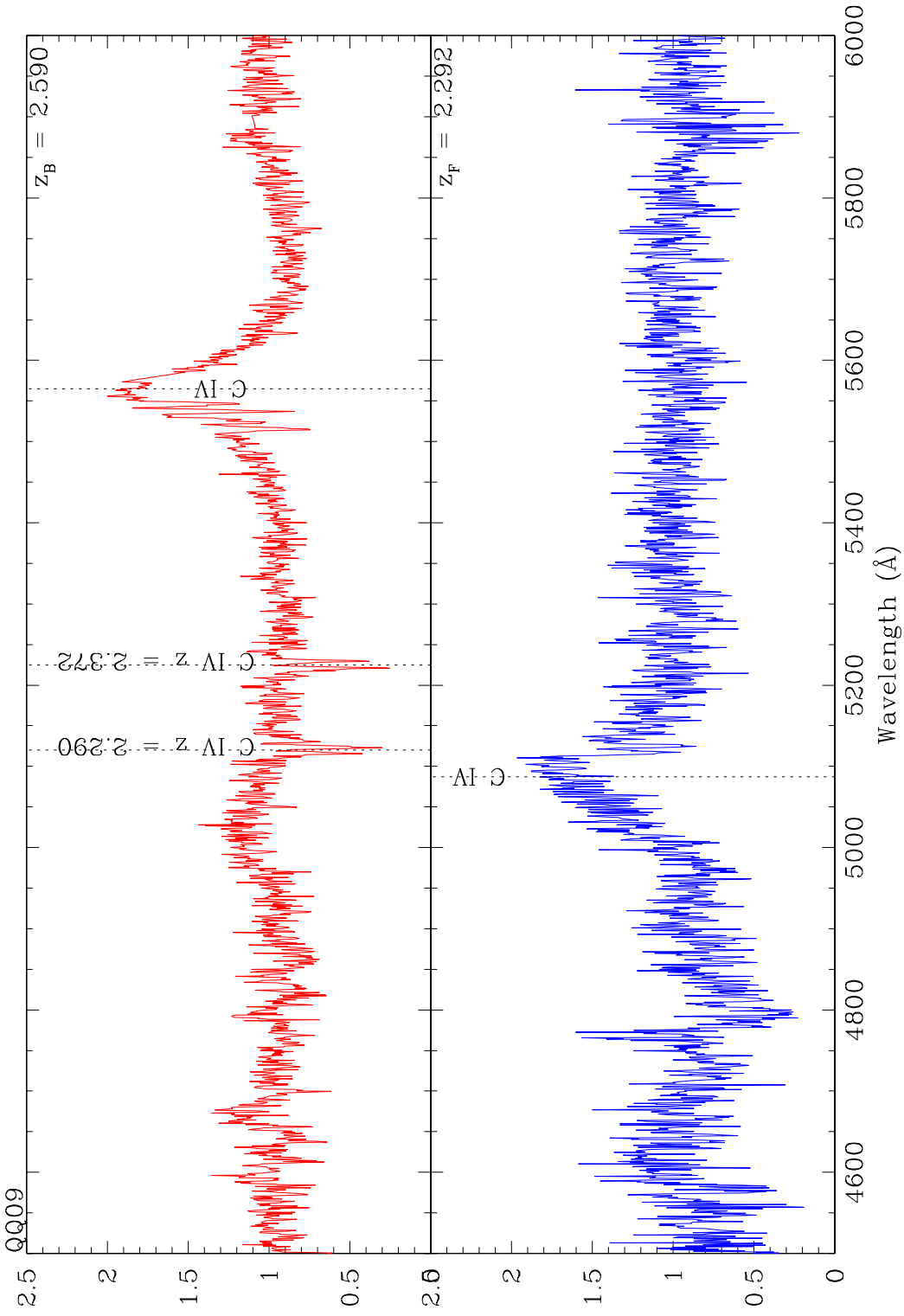

Figure 13. Spectra of pair QQ09.

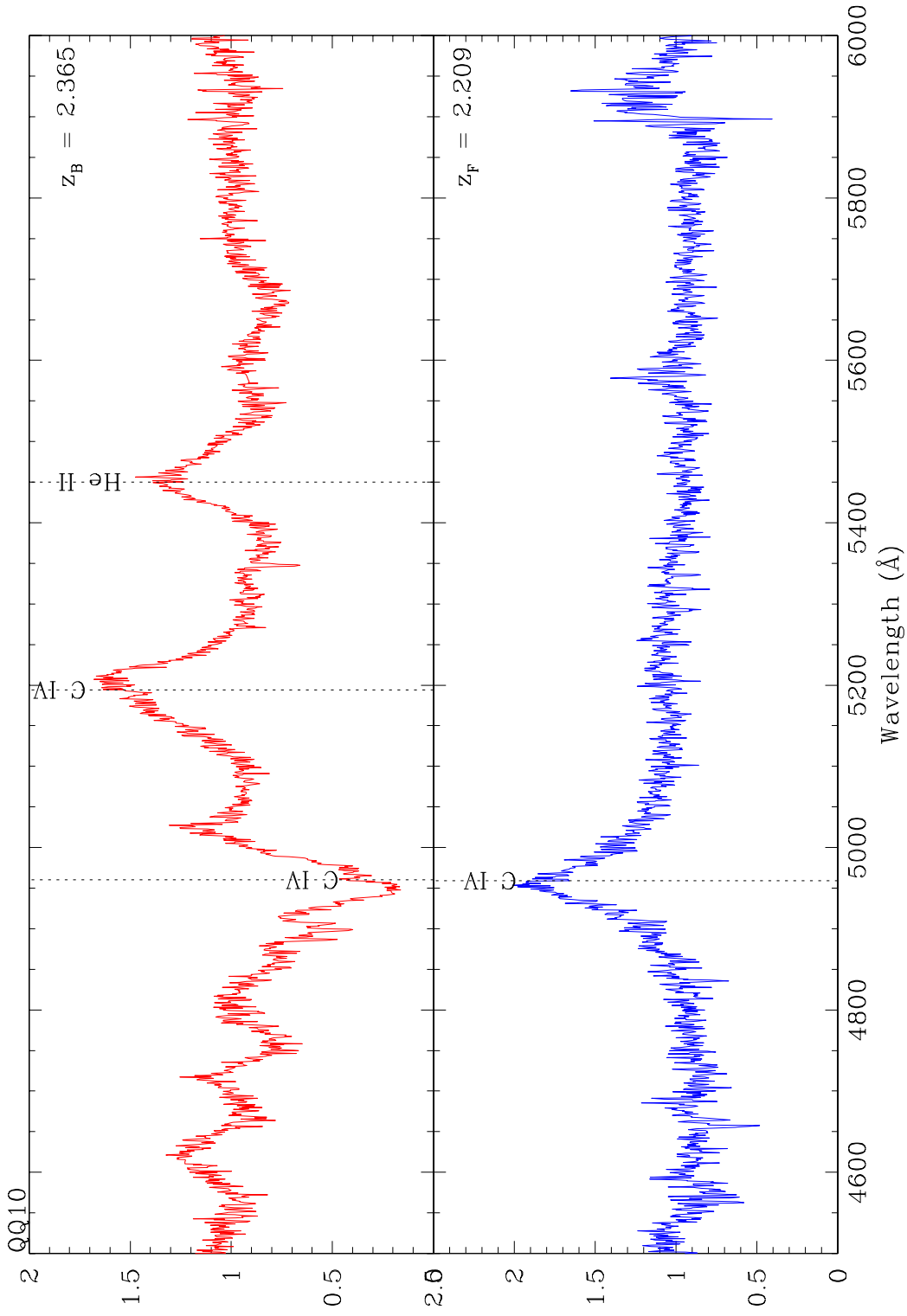

Figure 14. Spectra of pair QQ10.

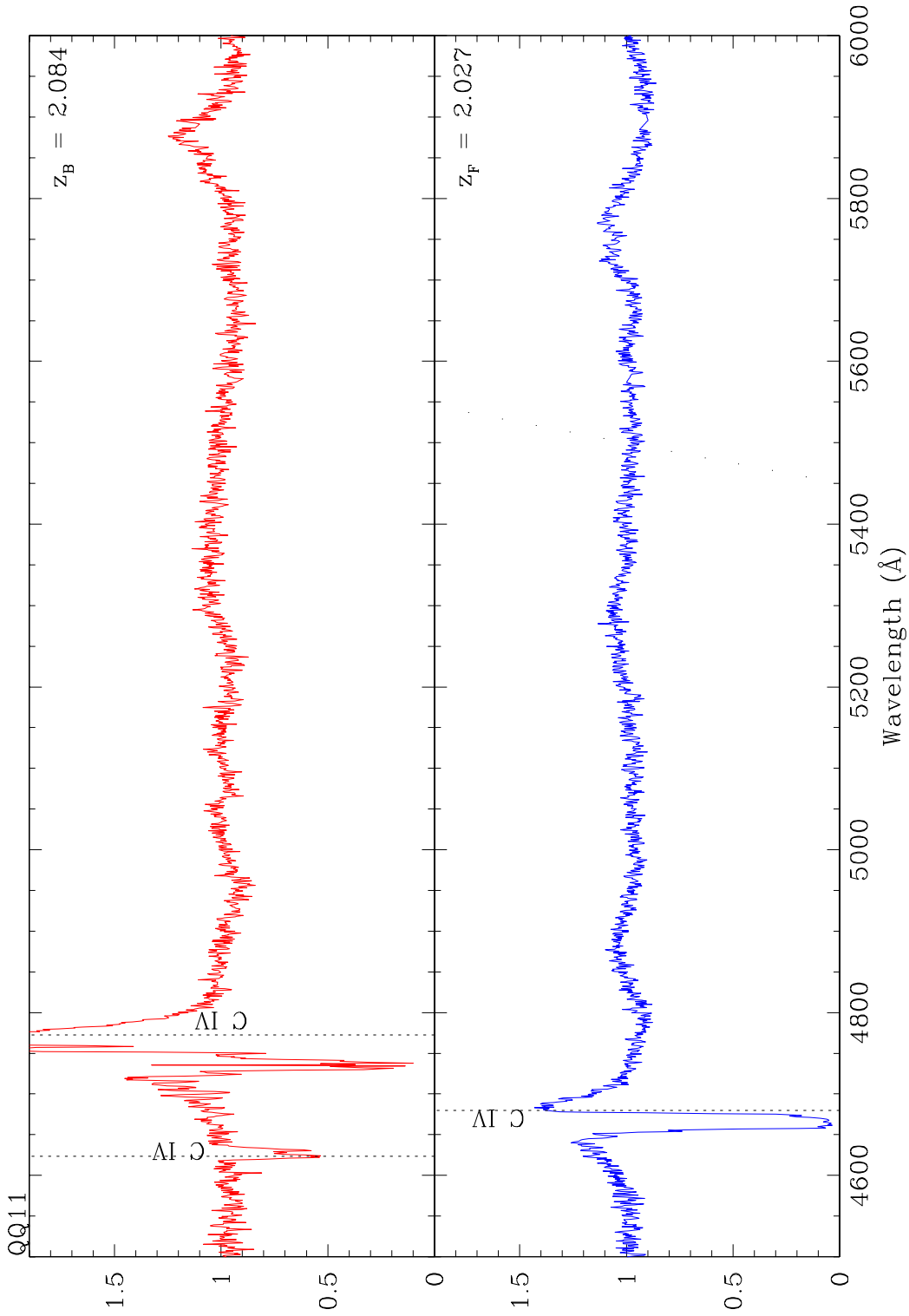

Figure 15. Spectra of pair QQ11.

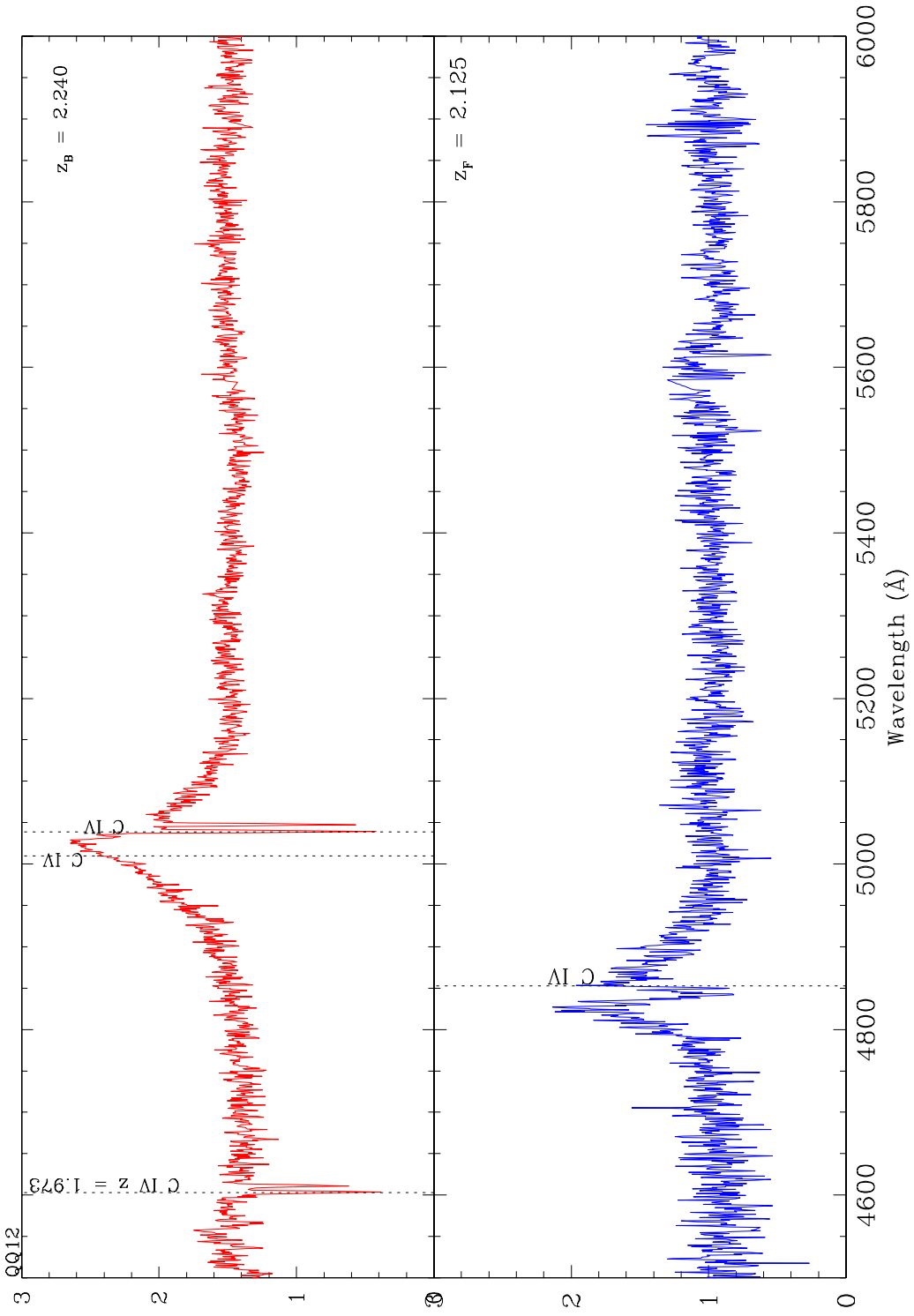

Figure 16. Spectra of pair QQ12.

This paper has been typeset from a TEX/LATEX file prepared by the author.

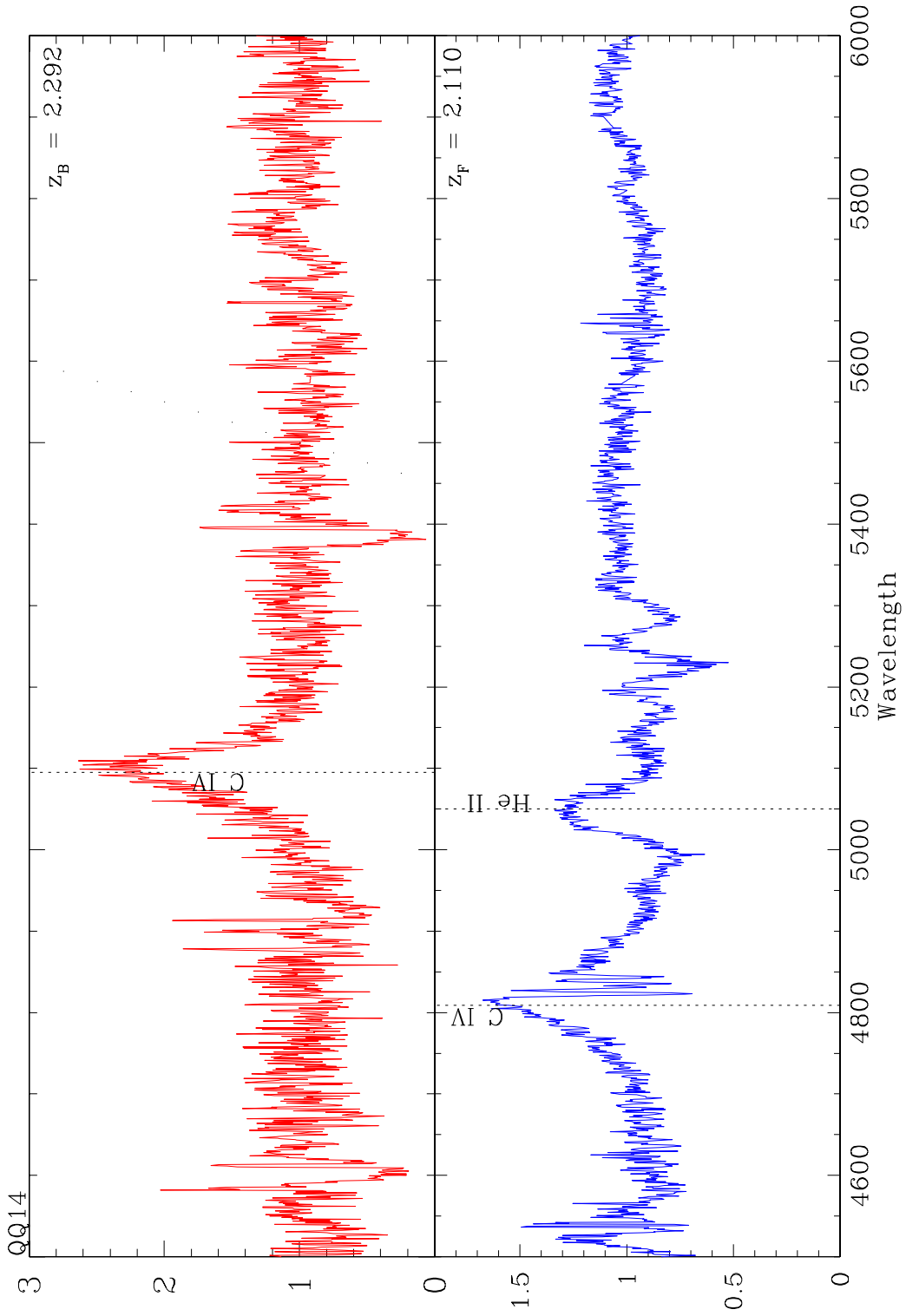

Figure 17. Spectra of pair QQ14.

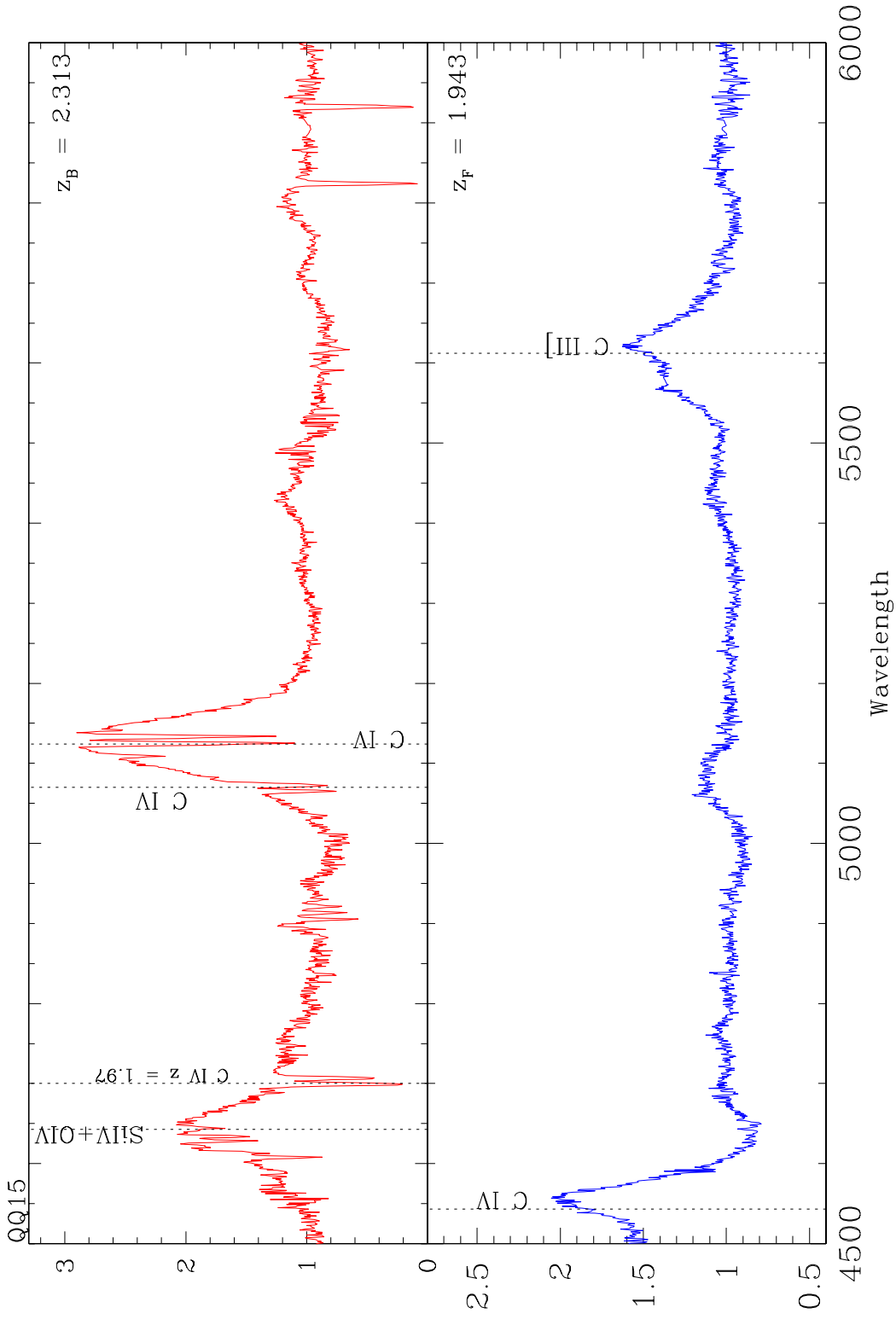

Figure 18. Spectra of pair QQ15.

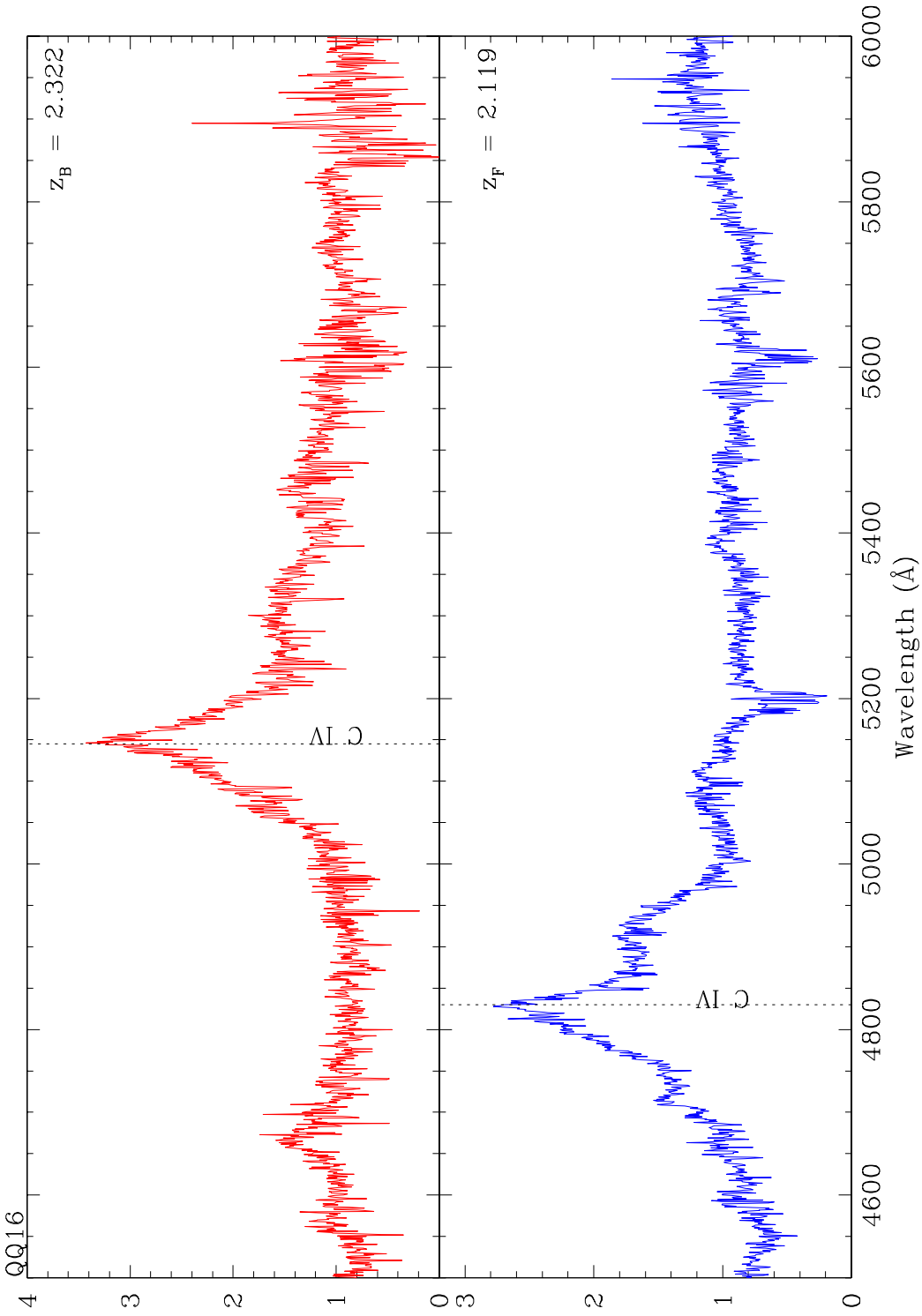

Figure 19. Spectra of pair QQ16.

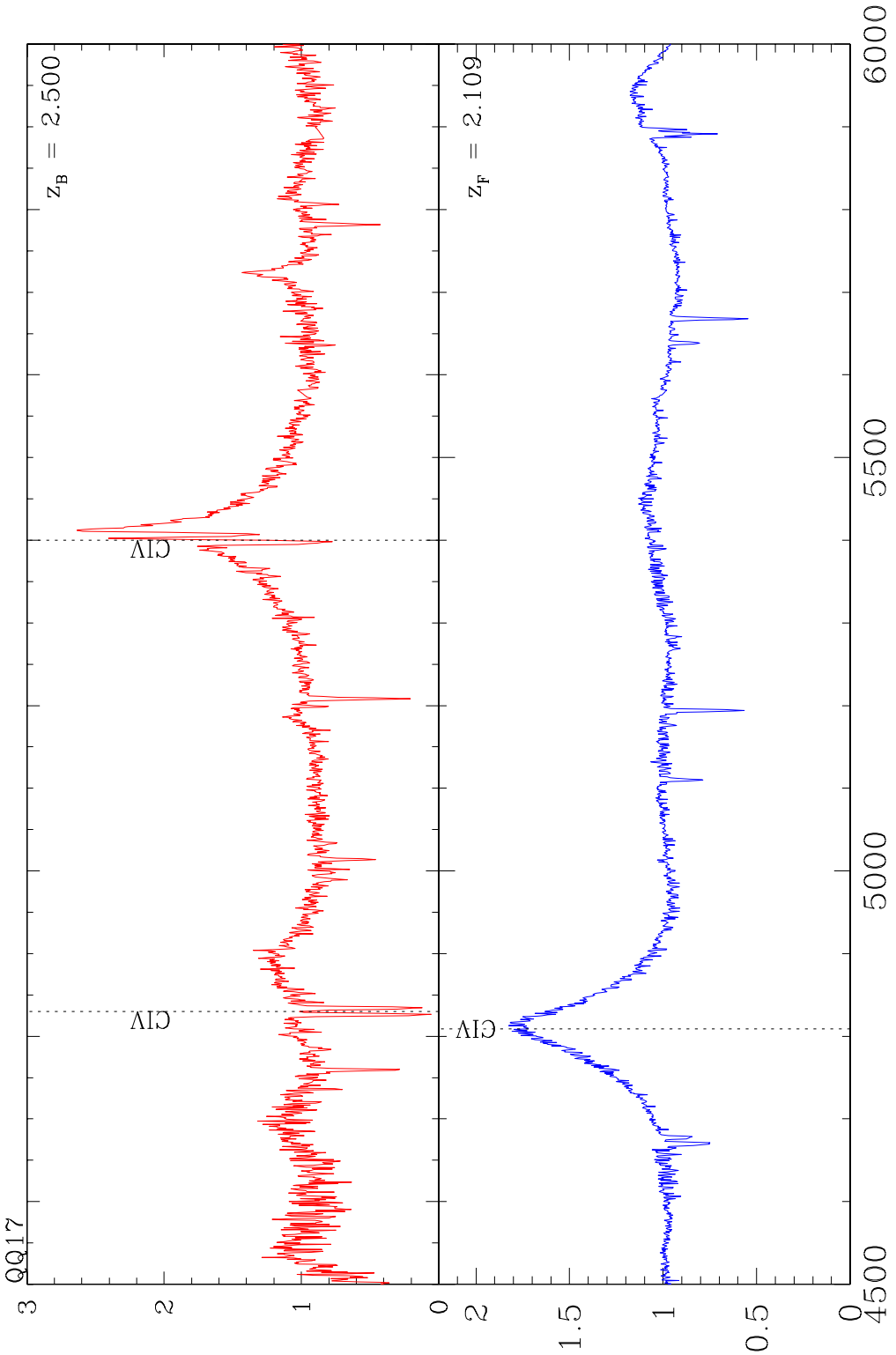

Figure 20. Spectra of pair QQ17.

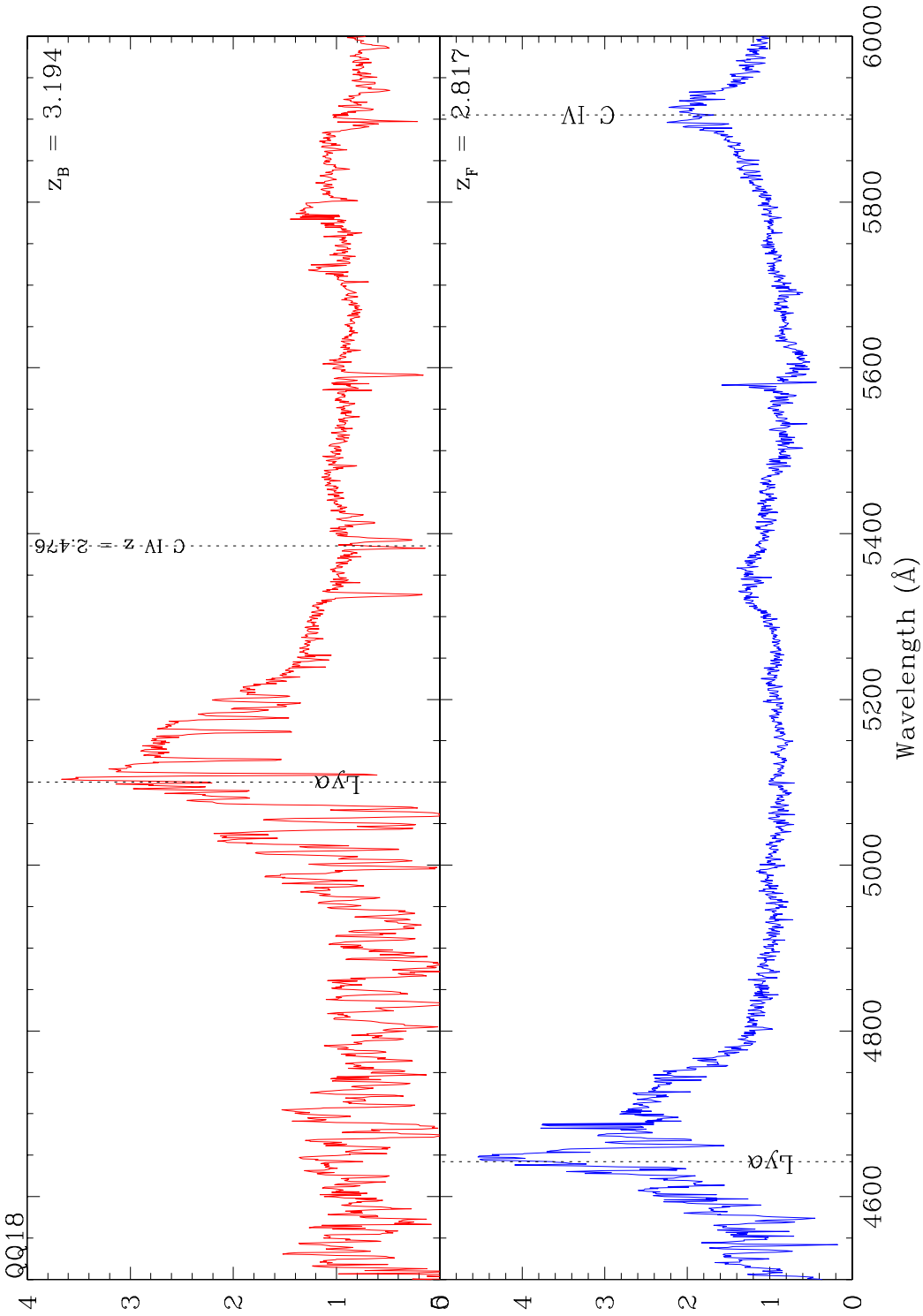

Figure 21. Spectra of pair QQ18.